Computers and Chemical Engineering 112 (2018) 154–164

Contents lists available at ScienceDirect

Computers and Chemical Engineering

journal homepage: www.elsevier.com/locate/compchemeng

A new framework of global sensitivity analysis for the chemical kinetic model using PSO-BPNN

Jian An, Guoqiang He, Fei Qin*, Rui Li, Zhiwei Huang

Science and Technology on Combustion, Internal Flow and Thermal-structure Laboratory, Northwestern Polytechnical University, Xi'an, Shaanxi, 710072, PR China

ARTICLE INFO

Article history:
Received 3 March 2017
Revised 14 January 2018
Accepted 1 February 2018
Available online 8 February 2018

Keywords:
Global sensitivity analysis
High dimensional model representation (HDMR)
Back-propagation neural network (BPNN)
Particle swarm optimization (PSO)
Garson method
PaD method

ABSTRACT

Global sensitivity analysis is a tool that primarily focuses on identifying the effects of uncertain input variables on the output and has been investigated widely in chemical kinetic studies. Conventional variance-based methods, such as Sobol' sensitivity estimation and high dimensional model representation (HDMR) methods, are computationally expensive. To accelerate global sensitivity analysis, a new framework that combines a variance-based (Wu's method) and two ANN-based sensitivity analysis methods (Weights and PaD) was proposed. In this framework, a back-propagation neural network (BPNN) methodology was applied, which was optimized by a particle swarm optimization (PSO) algorithm and trained with original samples. The Wu's method and Weights and PaD methods were employed to calculate sensitivity indices based on a well-trained PSO-BPNN. The convergence and accuracy of the new framework were compared with previous methods using a standard test case (Sobol' g-function) and a methane reaction kinetic model. The results showed that the new framework can greatly reduce the computational cost by two orders of magnitude, as well as guaranteeing accuracy. To take maximum advantage of the new framework, a four-step process combining the advantages of each method was proposed and applied to estimate the sensitivity indices of a C_2H_4 ignition model. The sensitivity indices of the more complex model could be implemented easily with good accuracy when the four-step process is followed

1. Introduction

Detailed chemical kinetic modeling of pure or mixed fuels enables an in-depth understanding of ignition and combustion processes. However, for a complex chemical kinetic model consisting of hundreds or even thousands of input parameters, including reaction rate coefficients, thermodynamic conditions and transport parameters, it is difficult to accurately determine the importance or influence of each parameter. Therefore, sensitivity analysis (SA) is often employed to identify the impact of variations and rank the importance of the input parameters (Paruggia, 2006). The sensitivity analysis mainly includes local sensitivity analysis (LSA) and global sensitivity analysis (GSA). LSA aims to explore the response of the model output to a small variation around a reference point (Haaker and Verheijen, 2004), while GSA focuses on the entire variation range of the variable. If the model has strong nonlinear effects, LSA will depend on the choice of the reference point and may produce misleading results. Therefore, GSA is more suitable for highly nonlinear models, and more current studies are using GSA methods instead of LSA. Many methods for GSA are available, such as moment-independent importance measures (Borgonovo, 2007; Chun et al., 2000; Liu et al., 2006), variance-based methods (Alis and Rabitz, 2001; Li et al., 2002; Rabitz and Alis, 1999; Sikorski et al., 2016) and artificial neural network (ANN)-based methods (Cao and Qiao, 2007; Lee et al., 2015; Olden et al., 2004; Sellitto, 2017), among which variance- and ANN-based methods have a general applicability because they can reflect the effect of the input variables on the output response. In this study, we focused on these two methods, which are introduced in the following paragraphs in detail.

The basic idea of variance-based methods is to decompose the total variance of the output D into orders of partial variance contribution; i.e.,

$$D = \sum_{i=1}^{n} D_i + \sum_{1\le i<j\le n}^{n} D_{ij} + \cdots + D_{12\ldots n} \quad (1)$$

where D_i is first order or main variance contribution of the ith input, D_{ij} is the second order variance contributed by interactions between the ith input and jth input, and $D_{12\ldots n}$ is a higher order variance contribution. Thus, a variance-based global sensitivity index can be obtained; e.g., the first-order sensitivity index S_i is de-

* Corresponding author.
E-mail address: qinfei@nwpu.edu.cn (F. Qin).

https://doi.org/10.1016/j.compchemeng.2018.02.003
0098-1354/

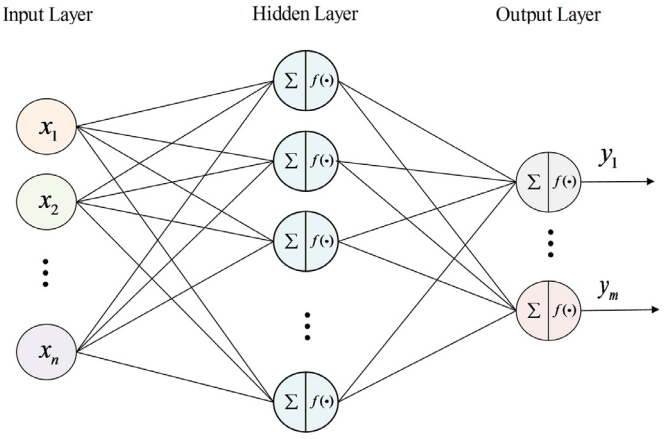

Fig. 1. Three typical layers in a BPNN with a single hidden layer.

fined as

$$S_i = D_i/D \tag{2}$$

However, for a complex model, there is no mathematical expression to calculate the variance or partial variance. Hence, Sobol' proposed a method based on Monte Carlo sampling to integrate partial variances (Sobol, 1990, 2001), which is able to estimate all order variances (i.e., V_i –$V_{12....n}$) and further obtain accurate results for sensitivity indices. Nevertheless, Sobol's method requires numerous samples to perform integration; thus, the high computational cost hinders its application in highly nonlinear chemical kinetic models. Wu et al., (2012) has provided an optimized method to improve the computing efficiency and convergence of Sobol's method. A brief theoretical introduction of Wu's method is provided in Section 2.1.2. Compared with Sobol's method, this method requires only half of the samples and has the same precision.

To further speed up the calculation, assuming negligible higher order interactive effects, a random sampling high dimensional model representations (RS-HDMR) utilizes an orthonormal polynomial function as the surrogate model of the original model and provides a straightforward approach to construct the low order decomposition expression (Rabitz and Alis, 1999). To improve the performance of RS-HDMR, several optimization methods have been proposed. Li et al. (2002) developed several practical approaches to construct orthonormal polynomials using a minimization process and Monte Carlo integration (named as DMC-HDMR hereafter). Furthermore, a threshold was introduced by Ziehn and Tomlin (2008a, 2008b) to exclude unimportant component functions and automatically determine the best order of the polynomials (named as Optimized-HDMR hereafter). Moreover, a user-friendly program has been developed based on the RS-HDMR method and its optimized extensions to improve usability (Ziehn and Tomlin, 2009). It is worth mentioning that although HDMR-like methods have better computational performance compared with Sobol's method, they may cause instability; for example, by increasing the risk of missing important terms.

As for ANN-based methods, first, ANN can be used as a surrogate model for effectively dealing with nonlinear relationships. For this reason, ANN has been applied for reliability analysis (Hao et al., 2012; Ruiz et al., 2001), classification (Ali et al., 2015) and modeling (Ahmad et al., 2004; Cui et al., 2012; Zorzetto et al., 2000). The most popular type of ANN is a back-propagation artificial neural network (BPNN) because of its excellent training speed (Rumelhart et al., 1986). As shown in Fig. 1, a typical BPNN consists of the following three layers: 1) input layer, 2) hidden layer and 3) output layer. These layers are connected by weights and biases that decide the importance of each neural. During the training process, the inputs are passed into the feed-forward algorithm and the output errors are propagated backward to adjust the weights and biases.

However, at beginning of training, the values of the weights and biases are randomly chosen; thus, many optimization methods have been developed to choose initial values, such as evolutionary methods (Rigo et al., 2005), gene expression programming (GA) (Ferreira, 2006), simulated annealing (Da and Ge, 2005), and particle swarm optimization (PSO) (Cao et al., 2016; Lin et al., 2008; Xiao and Ye, 2009). Among these types, PSO methods have been extensively used because of their efficiency, which optimizes the initial values by randomly initializing with a swarm of particles and then searching the optimal and updating generations. It has been previously shown by others that BPNN coupled with PSO can achieve faster convergence and higher solution accuracy (Cao et al., 2016; Lin et al., 2008; Xiao and Ye, 2009).

Furthermore, ANN can also be used as a tool to assess the global sensitivity of the input parameters (Cao and Qiao, 2007; Lee et al., 2015; Nourani and Sayyah Fard, 2012; Olden et al., 2004; Sellitto, 2017). The following four methods have been proposed for the sensitivity analysis of variables in ANN: 1) the "Weights" method, which is based on computation using connection weights (Garson, 2012); 2) the 'PaD' and 'PaD2' methods (calculate first and second order sensitivity indices, respectively, hereinafter collectively called the 'PaD' method), which compute the derivatives of the ANN output (Dimopoulos et al., 1999; Dimopoulos et al., 1995; Gevrey et al., 2003); 3) the 'Perturb' method, which assesses the change in the mean square error of the ANN by adding a perturbation of the input variables (Scardi and Harding, 1999); and 4) the 'Stepwise' method, which estimates the change in the error value when adding or eliminating an input step (Balls et al., 1996). The "Weights" and "PaD" methods are proven to be reliable in many fields and are commonly used in the literature (Garson, 2012; Gevrey et al., 2006). Cao and Qiao (2007) used the "PaD" method to evaluate sensitivity in geotechnical engineering problems. Nourani and Sayyah Fard (2012) investigated the evaporation process in different climatological regimes, and the sensitivity analysis was performed with the "PaD" and "Weights" methods.

For the global sensitivity analysis of chemical kinetic models, many studies have been completed using variance-based methods; in contrast, studies on ANN-based methods have seldom been reported in the literature. Li et al., (2016) have introduced an ANN into sensitivity analysis to construct surrogate models of chemical kinetic models and generate a large number of samples. The proposed ANN-HDMR method is a double-layer surrogate model that couples the advantages of ANN and HDMR, and it shows better performance in convergence and stability compared with conventional RS-HDMR. However, they only used the ANN as a surrogate model to overcome the numerous sample requirements; ANN-based sensitivity analysis methods were not involved.

In this study, we propose a new framework that combines variance- and ANN-based methods to perform global sensitivity analysis on chemical kinetic models. The performance of the framework is assessed with Sobol's g-function as the benchmark and on ignition models. This paper is organized as follows. Section 2 introduces the theoretical methods. Section 3 briefly describes the test cases. Section 4 presents the results and discussion. Section 5 presents the paper's conclusions.

2. Theoretical methods

This section presents the main concepts related to the involved methods, which represent the necessary background for the comprehension of the different works available in the literature. First, suppose that an input-output system is described by the determin-

istic relation:

$$Y = f(\mathbf{x}) = f(x_1, x_2, \ldots x_n) \tag{3}$$

where $\boldsymbol{X}$ and $\boldsymbol{Y}$ are the input and output vectors respectively, x_i denotes the ith input, and n is the number of inputs.

2.1. Variance-based methods

2.1.1. Sobol' sensitivity estimation

If $f(\mathbf{x})$ is a square-integrable function, it is possible to represent $f(\mathbf{x})$ in the form:

$$f(\mathbf{x}) = f_0 + \sum_{i=1}^{n} f_i(x_i) + \sum_{1\le i<j\le n}^{n} f_{i,j}(x_i, x_j) + \cdots + f_{1,2\ldots n}(x_1, x_2, \ldots x_n) \tag{4}$$

where $f(\mathbf{x})$ represents a function defined in the unit hypercube, n is the number of inputs, f_0 is the zero-th order component function that represents the mean effect to $f(\mathbf{x})$, and $f_i(x_i)$ is the first order component function that represents the independent effects of x_i. $f_{i,j}(x_{ij})$ is the second order component function that represents the correlated effects of x_i and x_j; analogically, $f_{1,2\ldots n}(x_1, x_2, \ldots x_n)$ represents the nth correlated effects to $f(\mathbf{x})$ (McKay, 1997).

Sobol' (Sobol, 1990) has provided a Monte Carlo-based method to estimate partial variances. The mean value of $f(\mathbf{x})$ is estimated as

$$f_0 \approx \frac{1}{N}\sum_{m=1}^{N} f(x_m) \tag{5}$$

where N is the sample size of the Monte Carlo simulations. The total variance D and the first order partial variance D_i can be estimated as

$$D \approx \frac{1}{N}\sum_{m=1}^{N} f^2(x_m) - f_0^2 \tag{6}$$

$$D_i \approx \frac{1}{N}\sum_{m=1}^{N} f(\mathbf{u}_m^{-i}, x_{im}) f(\mathbf{v}_m^{-i}, x_{im}) - f_0^2 \tag{7}$$

In this formula, x_m are Monte Carlo samples, and $\mathbf{u}_m^{-i}$ and $\mathbf{v}_m^{-i}$ refer to different Monte Carlo samples generated on K^{n-1} (K^n minus the input parameter x_i). Furthermore, the second order partial variance D_{ij} can be estimated by

$$D_{ij} \approx \frac{1}{N}\sum_{m=1}^{N} f(\mathbf{u}_m^{-ij}, x_{im}, x_{jm}) f(\mathbf{v}_m^{-ij}, x_{im}, x_{jm}) - D_i - D_j - f_0^2 \tag{8}$$

Finally, the first order sensitivity index S_i can be calculated by Eq. (2) and the second order sensitivity index S_{ij} is defined as:

$$S_{ij} = D_{ij}/D \tag{9}$$

Eqs. (5)–(8) show that the sensitivity indices can be calculated as long as there are enough samples. Additionally, variance-based sensitivity indices are generally named Sobol' sensitivity indices.

2.1.2. Wu's method

For a complex model, numerous samples are required to obtain a stable result. Therefore, Wu et al. (2012) has provided an optimized method to reduce the sample requirements. The basic idea is to make the sampling–re-sampling processing 'smoother' by 'averaging'. To introduce Wu's method, the following notation is defined:

$$I_A = f(\mathbf{u}_m) \tag{10}$$

$$I_B = f(\mathbf{v}_m) \tag{11}$$

$$I_C^{(1)} = f(\mathbf{u}_m^{-i}, \mathbf{v}_m^{i}) \tag{12}$$

$$I_D^{(1)} = f(\mathbf{u}_m^{i}, \mathbf{v}_m^{-i}) \tag{13}$$

$$I_C^{(2)} = f(\mathbf{u}_m^{-ij}, \mathbf{v}_m^{ij}) \tag{14}$$

$$I_D^{(2)} = f(\mathbf{u}_m^{ij}, \mathbf{v}_m^{-ij}) \tag{15}$$

where $\boldsymbol{I}$ are notations used below; $\mathbf{u}_m$ and $\mathbf{v}_m$ refer to different Monte Carlo samples; $\mathbf{u}_m^i$, $\mathbf{u}_m^{ij}$, $\mathbf{v}_m^i$ and $\mathbf{v}_m^{ij}$ are the ith or ith and jth column of $\mathbf{u}_m$ and $\mathbf{v}_m$, $\mathbf{u}_m^{-i}$, $\mathbf{u}_m^{-ij}$, $\mathbf{v}_m^{-i}$ and $\mathbf{v}_m^{-ij}$ are formed by all the columns in $\mathbf{u}_m$ and $\mathbf{v}_m$ except the ith or ith and jth column. Based on the above-defined parameters, the mean value is estimated as:

$$f_0 \approx \frac{1}{2N}\sum_{s=1}^{N} f(I_A) + f(I_B) \tag{16}$$

The total variance D and the partial variance D_i and D_{ij} can be estimated as:

$$D \approx \frac{1}{2N}\sum_{s=1}^{N} (f^2(I_A) + f^2(I_B)) - f_0^2 \tag{17}$$

$$D_i = \frac{1}{2N}\sum_{s=1}^{N} f(I_A) f(I_C^{(1)}) + f(I_B) f(I_D^{(1)}) \tag{18}$$

$$D_{ij} = \frac{1}{2N}\sum_{s=1}^{N} f(I_A) f(I_C^{(2)}) + f(I_B) f(I_D^{(2)}) \tag{19}$$

The Sobol' sensitivity indices can be subsequently estimated by Eqs. (2) and (9).

2.1.3. DMC-HDMR method

HDMR is other method to improve the computational efficiency by using orthonormal polynomials to construct the HDMR expression (Li et al., 2002). Orthonormal polynomials are defined as:

$$\begin{aligned} &\varphi_1(x) = \sqrt{3}(2x-1), \\ &\varphi_2(x) = 6\sqrt{5}\left(x^2 - x + \frac{1}{6}\right), \\ &\varphi_3(x) = 20\sqrt{7}\left(x^3 - \frac{3}{2}x^2 + \frac{3}{5}x - \frac{1}{20}\right) \\ &\ldots \end{aligned} \tag{20}$$

Thus, Eq. (4) can be expressed as

$$f(\mathbf{x}) = f_0 + \sum_{i=1}^{n}\sum_{r=1}^{k} \alpha_r^i \varphi_r(x_i) + \sum_{1\le i<j\le n} \sum_{p=1}^{k1}\sum_{q=1}^{k2} \beta_{pq}^{ij} \varphi_p(x_i)\varphi_q(x_j) \tag{21}$$

where only the first and second order are considered, which can provide a satisfactory approximation, and the coefficients α_r^i and β_{pq}^{ij} are calculated by the Monte Carlo integration (Alis and Rabitz, 2001; Li et al., 2002):

$$\alpha_r^i \approx \frac{1}{N}\sum_{m=1}^{N} f(x_m)\varphi_r(x_{im}) \tag{22}$$

$$\beta_{pq}^{ij} \approx \frac{1}{N}\sum_{m=1}^{N} f(x_m)\varphi_p(x_{im})\varphi_q(x_{jm}) \tag{23}$$

where N is the sample size. Consequently, the total variance D and partial variances D_i and D_{ij} can be calculated by

$$D \approx \frac{1}{N}\sum_{s=1}^{N} f^2(x_m) - f_0^2 \tag{24}$$

$$D_i = \sum_{r=1}^{k} (\alpha_r^i)^2 \tag{25}$$

$$D_{ij} = \sum_{p=1}^{k1}\sum_{q=1}^{k2} (\beta_{pq}^{ij})^2 \tag{26}$$

Finally, the Sobol' sensitivity indices can be obtained from Eqs. (2) and (9).

2.1.4. Optimized-HDMR method

The primary approaches for Optimized-HDMR are similar to DMC-HDMR Eqs. (20)–((26)). Some revised algorithms are introduced to improve the efficiency and usability, such as the control variate (Li and Rabitz, 2006; Li et al., 2003), automatically chosen order (Ziehn and Tomlin, 2008a) and excluding unimportant terms (Ziehn and Tomlin, 2008b). More information on the algorithms can be found in the abovementioned references.

2.2. ANN-based methods

An ANN has the ability to establish a nonlinear relationship between two data spaces. Generally, an ANN with an N-neuron input layer, an L-neuron hidden layer and an M-neuron output layer was considered in this section. After training, an ANN can provide a mathematical relationship between the multi-dimensional inputs and outputs as:

$$X \rightarrow Y \tag{27}$$

where the output of one neuron is calculated by the following equation:

$$o_i = \phi(net_i) = \phi\left(\sum_{j=1}^{N} w_{ij}x_j + \theta_i\right) \tag{28}$$

where o_i and θ_i represent the response and bias of the ith neuron, respectively. $w = (w_{ij})_{N\times L}$ and $v = (v_{jk})_{L\times M}$ are the matrix of the connection weights between the input and hidden neurons and the output and hidden neurons, respectively, and $\phi(\cdot)$ denotes the activation function of the layers. The output from one neuron provides the input for the neurons in the next layer. According to Eq. (28), the weights play an important role in the calculation process and can be explained from a different perspective. On one side, the fitting precision depends on the weight values; thus, a reliable and effective method should be applied to calculate the weights. In contrast, one can see that the scalar weights determine the strength of each input's influence; therefore, the sensitivity and influence of an input can be estimated using the weights. Based on these two key points, a PSO algorithm was applied to optimize the weights in this study; the Weights and PaD methods were introduced to analyze the global sensitivity.

2.2.1. Weights method

To identify the GSA capacities of an ANN, the Weights sensitivity analysis was applied to assess the relative contribution and roles of the input variables. The Weights method was proposed by Garson (2012). The sensitivity indices of the input variance Q_k^i were determined by the following equation:

$$Q_k^i = \frac{\sum_{j=1}^{L}(|w_{ij}v_{jk}|/\sum_{r=1}^{N}|w_{rj}|)}{\sum_{i=1}^{N}\sum_{j=1}^{L}(|w_{ij}v_{jk}|/\sum_{r=1}^{N}|w_{rj}|)} \tag{29}$$

It is noteworthy that Q_k^i is representative of the contribution of all input variables, including the second or higher order coupling effects.

2.2.2. PaD and PaD2 method

The PaD and PaD2 methods were developed by Dimopoulos et al. (1995, 1999) and are used to study the sensitivity of a single variable and two-way variables based on ANN. The PaD indices can be calculated as follows:

$$s_i^t = s\sum_{j=1}^{L} w_{ij}v_{j1}f_j^t(1-f_j^t) \tag{30}$$

$$S_i = \frac{\sum_{t=1}^{T}(s_i^t)^2}{\sum_{i=1}^{N}\sum_{t=1}^{T}(s_i^t)^2} \tag{31}$$

The S_i values allow classification of the variables according to their increasing contribution to the output variable. Based on an ideal PaD method, PaD2 can be obtained as follows:

$$s_{ik}^t = s_2\sum_{j=1}^{L} w_{ij}v_{j1}f_j^t(1-f_j^t)\sum_{j=1}^{L} w_{kj}v_{j1}f_j^t(1-f_j^t) + s_1\sum_{j=1}^{L} w_{ij}w_{kj}v_{j1}f_j^t(1-f_j^t)(1-2f_j^t) \tag{32}$$

$$S_{ij} = \frac{\sum_{t=1}^{T}(s_{ik}^t)^2}{\sum_{\substack{i=1\\k=i+1}}^{N}\sum_{t=1}^{T}(s_{ik}^t)^2} \tag{33}$$

The S_{ij} values refer to the second order sensitivity of the inputs. For simplicity, PaD and PaD2 are collectively called the PaD method hereafter.

2.3. New global sensitivity analysis framework

Fig. 2 shows a schematic diagram of the computational process for the conventional methods and the new global sensitivity analysis framework for the chemical kinetic model.

In this work, a single hidden layer BPNN was employed in the new framework because of its excellent training speed (Rumelhart et al., 1986). A PSO algorithm was chosen to optimize the initial values of the weights when training starts. PSO is a population-based optimization algorithm based on a simulation of the social behaviors of bird flocks, fish schools and insect swarms. The system is randomly initialized with a swarm of particles that are potential solutions and then searches the optimal and updated generations. A complete algorithm and more details on PSO-based BPNN can be found in the literature (Geethanjali et al., 2008; Lin et al., 2008; Xiao and Ye, 2009).

The new framework process is as follows: 1) generating a small number of samples using the original chemical kinetic models, which are called the original samples hereafter; 2) training the PSO-BPNN using the original samples and finally obtaining a well-trained BPNN; and 3) analyzing the global sensitivity using an ANN-based method (Weights and PaD methods, introduced in Section 2.2.1 and 2.2.2) or a variance-based method (Wu's method, introduced in Section 2.1.2). These three aims are called PSO-BPNN-Weights, PSO-BPNN-PaD and PSO-BPNN-Wu, respectively. Finally, the global sensitivity indices and the parameter importance order can be obtained.

As shown in Fig. 2, conventional HDMR methods (i.e., RS-HDMR, DMC-HDMR and Optimized-HDMR) use samples that are generated by original models to construct HDMR expression

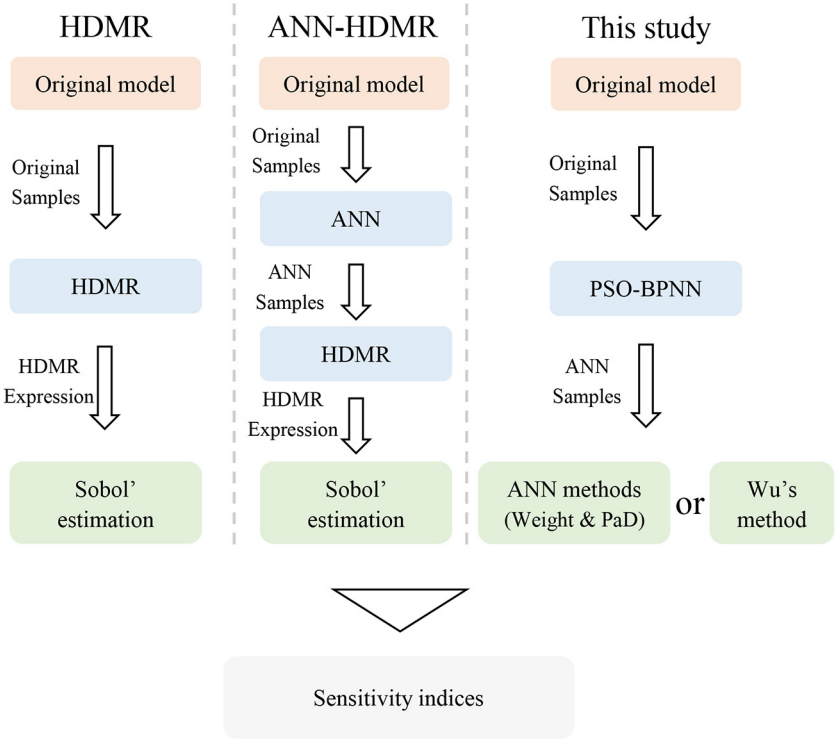

Fig. 2. Schematic diagram of the computational processes for conventional HDMR, ANN-HDMR and the new framework.

(Eq. (21)) and then use Sobol' sensitivity estimation (Eqs. (24)–(26)) to calculate the sensitivity indices. To overcome the numerous original samples requirement, an ANN trained by a small number of original samples was used as a surrogate model to further generate ANN samples for HDMR, i.e., ANN-HDMR. For the new framework, the HDMR process was omitted to accelerate the calculations, while an ANN became a key layer to obtain sensitivity indices. Note that ANN-based sensitivity indices are different from variance-based indices due to different algorithms. Thus, Wu's method is incorporated into the framework to calculate the Sobol' sensitivity indices and analyzed in comparison with the conventional HDMR methods.

3. Test cases

In this section, three cases were used to illustrate the performance of the new framework. Two cases are based on the Sobol' g-function, while the third one is a kinetic model of CH_4 ignition.

3.1. Sobol' g-function

The Sobol' g-function was introduced by Saltelli and Sobol (1995) and was defined as:

$$f(x) = \prod_{i=1}^{n} g_i(x_i) \tag{34}$$

$$g_i(x_i) = \frac{|4x_i - 2| + a_i}{1 + a_i}, a_i \geq 0 \tag{35}$$

where a_i is a constant and x_i is uniformly distributed from [0, 1]. Because the Sobol' g-function has analytical solutions, it is widely used to verify the accuracy of other methods.

3.2. Premixed CH_4 ignition model

Ignition delay time is an important combustion property. The CH_4 system is relatively small, which makes it easy to generate numerous original samples. A CH_4 ignition model updated by Smith et al., (1999) was used and can be found in Supplementary Materials S2. The ignition delay time for the CH_4/air system at T = 1000 K and p = 1 atm was chosen as a test target.

4. Results and discussion

In this section, the performance of the new framework and conventional methods, in terms of their computational efficiency, accuracy and usability, were compared using the test cases introduced in Section 3. To estimate the performance of the different methods, the computational efficiency was measured by the total CPU time cost and the accuracy and convergence were measured by an error function defined as:

$$error = \sum |S_i - S_i^a| + \sum |S_{ij} - S_{ij}^a| \tag{36}$$

In this equation, S_i and S_{ij} are calculated as the first and second order sensitivity indices and S_i^a and S_{ij}^a represent their analytical values, respectively.

4.1. Sobol' g-function

To make comparisons with previous studies (Li et al., 2016), two cases with a_i = (4.5, 4.5, 1, 0, 1, 9, 0, 9) (case 1) and a_i = (5000, 5500, 6000, 6500, 7000, 7500, 8000, 8500) (case 2), which are commonly used, were studied. According to the g-function algorithm, the greater the a_i value, the smaller the variance from the corresponding input x_i. For the original samples, a Sobol' quasi-random sequence was used. For Optimized-HDMR, the maximum polynomial orders for the first and second component functions were set as 10 and 5, respectively.

4.1.1. Variance-based method

In the case of a_i = (4.5, 4.5, 1, 0, 1, 9, 0, 9), both the first and second order sensitivity indices were obtained by different methods. Table 1 lists all the first order and the top five second order

Table 1
The important first and second order sensitivity indices for the Sobol' g-function with a_i = (4.5, 4.5, 1, 0, 1, 9, 0, 9) using Optimized-HDMR, ANN-HDMR and PSO-BPNN-Wu.S_i represents the first order sensitivity index of parameter x_i. S_{ij}represents the second order sensitivity index of parameter x_i and x_j. $\Sigma(S_i)$ is the sum of all the first order sensitivity indices. $\Sigma(S_{i,j})$ is the sum of all the second order sensitivity indices. $\sum(S_i + S_{i,j})$ is the sum of all the first and second order sensitivity indices. The error is calculated according to Eq. (36).

N	Optimized-HDMR (Li et al., 2016)		ANN-HDMR (Li et al., 2016)		PSO-BPNN-Wu			Analytical
	4096	8192	4096	8192	1024	2048	4096	
S_1	0.0122	0.0103	0.0092	0.0095	0.0099	0.0096	0.0098	0.0096
S_2	0.0095	0.0097	0.0094	0.0096	0.0100	0.0087	0.0096	0.0096
S_3	0.0729	0.0724	0.0712	0.0724	0.0751	0.0715	0.0729	0.0727
S_4	0.2784	0.2865	0.2903	0.2897	0.2959	0.2912	0.2901	0.2906
S_5	0.0723	0.0718	0.0714	0.0725	0.0741	0.0746	0.0723	0.0727
S_6	0.0000	0.0027	0.0028	0.0029	0.0030	0.0027	0.0030	0.0029
S_7	0.2866	0.2866	0.2920	0.2898	0.2953	0.2918	0.2909	0.2906
S_8	0.0036	0.0036	0.0027	0.0028	0.0030	0.0024	0.0028	0.0029
$\Sigma(S_i)$	0.7289	0.7437	0.7491	0.7491	0.7663	0.7525	0.7514	0.7516
$S_{4,7}$	0.0919	0.0926	0.0949	0.0942	0.0934	0.0950	0.0959	0.0969
$S_{3,4}$	0.0245	0.0238	0.0231	0.0235	0.0228	0.0234	0.0238	0.0242
$S_{3,7}$	0.0251	0.0238	0.0233	0.0234	0.0231	0.023	0.0237	0.0242
$S_{4,5}$	0.0246	0.0233	0.0232	0.0236	0.0232	0.0231	0.0236	0.0242
$S_{5,7}$	0.0244	0.0233	0.0234	0.0235	0.0229	0.0235	0.0238	0.0242
$\Sigma(S_{i,j})$	0.2138	0.2161	0.2140	0.2149	0.2104	0.2122	0.2170	0.2209
$\Sigma(S_i + S_{i,j})$	0.9427	0.9598	0.9631	0.9640	0.9764	0.9647	0.9684	0.9725
Error	0.0381	0.0180	0.0137	0.0106	0.0235	0.1238	0.0087	0.0000

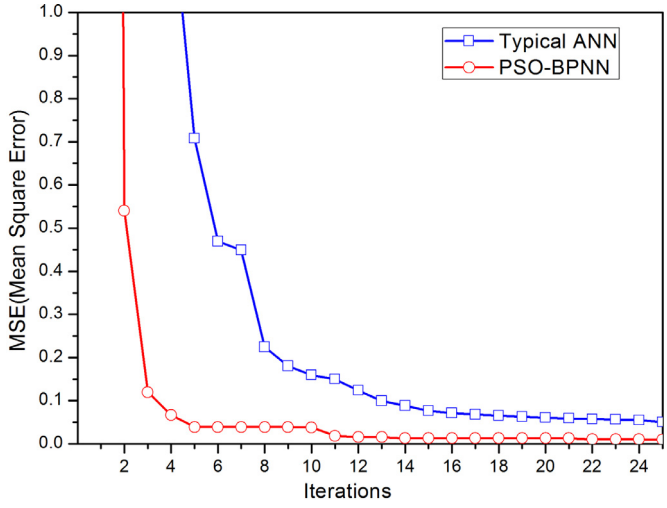

Fig. 3. The mean square error tendency versus the training iterations.

sensitivity indices using Optimized-HDMR, ANN-HDMR, and PSO-BPNN-Wu. The Optimized-HDMR and ANN-HDMR data come from Li et al., (2016). The number of original samples for PSO-BPNN was set as 1024, 2048, and 4096, respectively. A more detailed PSO-BPNN configuration that includes the number of hidden layers is provided in Supplementary Materials S1.

After training (mean square of errors (MSE) for the whole training data set was less than 1×10^{-10}), the HDMR samples were easily obtained by using BPNN. In total, 0.2 million BPNN generated samples are enough to generate stable results. Fig. 3 shows the change in the mean square error tendency during the training iterations. It is obvious that the PSO-BPNN converges faster than a typical ANN. Weights and biases can be obtained quickly and steadily using the PSO algorithm. By comparing the PSO-BPNN-Wu with Optimized-HDMR and ANN-HDMR methods, we observed that PSO-BPNN-Wu only requires 1024 samples to reduce the error to below 5%, while Optimized-HDMR and ANN-HDMR required 4096 and 2048 samples, respectively, to obtain the same accuracy. This result suggests that PSO-BPNN can reduce the original samples requirement and maintain the accuracy.

In case 2, according to the analytical solutions, the second and higher order terms can be neglected; therefore, only the first order sensitivity indices were calculated. Table 2 lists all the sensitivity indices with various sample sizes using different methods. Although the PSO algorithm did not reduce the sample size in this case (because the sample size is small enough), it reduced the error at the same sample size.

4.1.2. Weights method

Table 3 shows that the sensitivity indices varied with the original sample sizes using the Weights method. It is important to understand the meaning of the Weights sensitivity indices. These sensitivity indices based on the BPNN weights are the total variance contribution of each input, are similar to S_{Ti} the in Sobol' method, and are defined as follows:

$$S_{Ti} = S_i + \sum_{j>i} S_{ij} + \sum_{l>j>i} S_{ijl} + \cdots + S_{12\ldots k} \tag{37}$$

However, the values of the Weights sensitivity indices do not converge to S_{Ti} because of the different algorithms. Therefore, the correlation coefficients R between the Weights and Sobol' sensitivity indices were introduced to evaluate its performance, which can be calculated by the following equation:

$$R = \frac{\sum_{i=1}^{N}(X_i - \overline{X})(Y - \overline{Y})}{\sqrt{\sum_{i=1}^{N}(X_i - \overline{X})^2}\sqrt{\sum_{i=1}^{N}(Y_i - \overline{Y})^2}} \tag{38}$$

The analytical solutions for S_{Ti} based on Sobol' method and the correlation coefficients are listed. By combining Table 3 with Fig. 4, one can see that there is a strong correlation between the two methods, as the correlation coefficient can be as high as 99% for 4096 samples. This result shows that these two methods follow similar trends. For the influence of the samples, 1024 original samples are enough to generate a correct ranking, while 4096 original samples are required to obtain a converged result.

Table 4 lists the eight Weights indices for case 2. It illustrates that the correlation coefficients increase with the sample size. In total, 256 samples are enough to obtain a correct ranking and 1024 samples can raise the correlation coefficient to 99%.

These two cases show that the Weights method is an available method to obtain the total sensitivity indices from the input. For systems with interactive effects, the sensitivity indices have similar trends and ranking.

Table 2
The important first and second order sensitivity indices for the Sobol' g-function with a_i = (5000, 5500, 6000, 6500, 7000, 7500, 8000, 8500) using Optimized-HDMR, ANN-HDMR and PSO-BPNN-Wu.

N	Optimized-HDMR (Li et al., 2016)		ANN-HDMR (Li et al., 2016)		PSO-BPNN-Wu			Analytical
	262,144	524,288	512	1024	256	512	1024	
S_1	0.2049	0.2069	0.2099	0.2096	0.2064	0.2072	0.2082	0.2081
S_2	0.1693	0.1710	0.1746	0.1718	0.1726	0.1748	0.1725	0.1720
S_3	0.1423	0.1437	0.1422	0.1436	0.1559	0.1453	0.1455	0.1446
S_4	0.1213	0.1224	0.1235	0.1259	0.1267	0.1254	0.1223	0.1232
S_5	0.1046	0.1056	0.1038	0.1058	0.1028	0.1049	0.1056	0.1062
S_6	0.0911	0.092	0.0941	0.0926	0.0925	0.0906	0.0931	0.0925
S_7	0.0800	0.0808	0.0802	0.0813	0.0776	0.0808	0.0805	0.0813
S_8	0.0709	0.0716	0.0705	0.0735	0.0647	0.0709	0.0723	0.0720
$\Sigma(S_i)$	0.9844	0.9939	0.9989	1.0041	0.9992	0.9999	1.0000	1.0000
Error	0.0156	0.0061	0.0136	0.0073	0.0319	0.0114	0.0049	0.0000

Table 3
The important first and second order sensitivity indices for the Sobol' g-function with a_i = (4.5, 4.5, 1, 0, 1, 9, 0, 9) using the PSO-BPNN-Weights method.

N	PSO-BPNN-Weights				Analytical
	512	1024	2048	4096	
S_{T1}	0.0547	0.0487	0.0747	0.0498	0.0139
S_{T2}	0.0786	0.0287	0.0619	0.0483	0.0139
S_{T3}	0.1303	0.0665	0.0850	0.1254	0.1003
S_{T4}	0.2194	0.3484	0.2831	0.3104	0.3678
S_{T5}	0.1104	0.1038	0.1141	0.1243	0.1003
S_{T6}	0.0494	0.0186	0.0494	0.0184	0.0042
S_{T7}	0.2821	0.3750	0.2944	0.3039	0.3678
S_{T8}	0.0751	0.0103	0.0474	0.0195	0.0042
R	0.9313	0.9803	0.9808	0.9958	1.0000

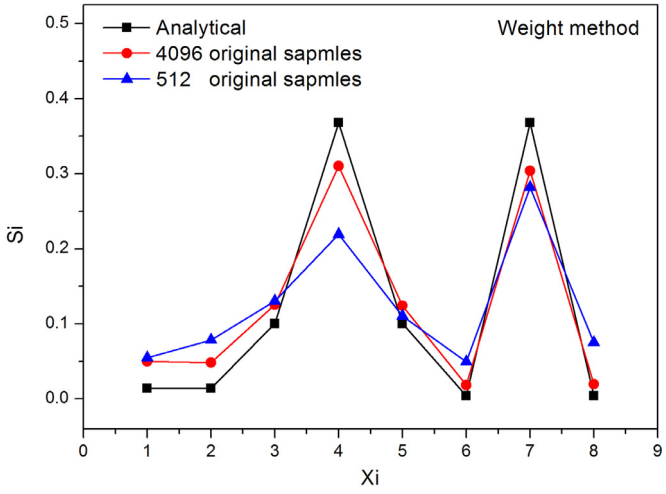

Fig. 4. Analytical Sobol' sensitivity indices and Weights method sensitivity indices with 4096 and 512 original samples.

Table 4
The important first and second order sensitivity indices for the Sobol' g-function with a_i = (4.5, 4.5, 1, 0, 1, 9, 0, 9) using the PSO-BPNN-Weights method.

N	PSO-BPNN-Weights			Analytical
	256	512	1024	
S_{T1}	0.1621	0.2636	0.2049	0.2081
S_{T2}	0.1532	0.1716	0.1776	0.1720
S_{T3}	0.1444	0.1491	0.1425	0.1446
S_{T4}	0.1204	0.0959	0.1303	0.1232
S_{T5}	0.1198	0.0941	0.1052	0.1062
S_{T6}	0.1093	0.0796	0.0931	0.0925
S_{T7}	0.1003	0.0732	0.0788	0.0813
S_{T8}	0.0906	0.0729	0.0675	0.0720
R	0.9648	0.9759	0.9964	1.0000

Table 5
The important first and second order sensitivity indices for the Sobol' g-function with a_i = (4.5, 4.5, 1, 0, 1, 9, 0, 9) using the PSO-BPNN-PaD method.

N	PSO-BPNN-PaD				Analytical
	512	1024	2048	4096	
S_1	0.0651	0.0015	0.0021	0.0023	0.0096
S_2	0.0712	0.0017	0.0020	0.0025	0.0096
S_3	0.0385	0.0113	0.0187	0.0207	0.0727
S_4	0.2687	0.5562	0.4148	0.4728	0.2906
S_5	0.1442	0.0124	0.0190	0.0211	0.0727
S_6	0.0844	0.0004	0.0007	0.0008	0.0029
S_7	0.2678	0.4157	0.5418	0.4790	0.2906
S_8	0.0601	0.0008	0.0009	0.0009	0.0029
R	0.8870	0.9284	0.9376	0.9618	1.0000
$S_{4,7}$	0.1298	0.9186	0.8877	0.8022	0.0969
$S_{3,4}$	0.1004	0.0226	0.0279	0.0444	0.0242
$S_{3,7}$	0.0618	0.0205	0.0202	0.0442	0.0242
$S_{4,5}$	0.0737	0.0147	0.0211	0.0424	0.0242
$S_{5,7}$	0.0843	0.0137	0.0271	0.0451	0.0242
R	0.8430	0.9951	0.9996	0.9999	1.0000

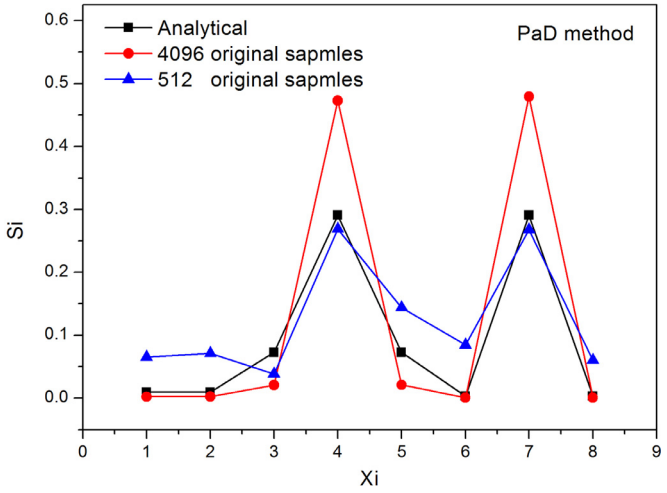

Fig. 5. Analytical Sobol' sensitivity indices and PaD method sensitivity indices with 4096 and 512 original samples.

4.1.3. PaD method

Compared with the Weights method, the PaD method can obtain first and second order sensitivity indices quickly. Similar to the Weights method, the correlation coefficients R between the PaD method and Sobol' sensitivity indices were used. As shown in Table 5 and Fig. 5. Both the first and second order sensitivity indices are highly correlated with the variance-based method, and the correlation coefficients increase with the number of sam-

Table 6
The important first and second order sensitivity indices for the Sobol' g-function with a_i = (5000, 5500, 6000, 6500, 7000, 7500, 8000, 8500) using the PSO-BPNN-PAD method.

N	PSO-BPNN-PAD			Analytical
	256	512	1024	
S_1	0.2051	0.2078	0.2083	0.2081
S_2	0.1768	0.1721	0.1736	0.1720
S_3	0.1452	0.1321	0.1445	0.1446
S_4	0.1335	0.1217	0.1235	0.1232
S_5	0.1088	0.1036	0.1054	0.1062
S_6	0.0885	0.0926	0.0911	0.0925
S_7	0.0846	0.0819	0.0820	0.0813
S_8	0.0575	0.0736	0.0717	0.0720
R	0.9897	0.9955	0.9999	1.0000

ples. The PaD method requires 4096 original samples to raise R to 99.99% and only 1024 to obtain a correct ranking. This result illustrates that the PaD method can generate the same sensitivity analysis results as the variance-based methods.

Because the second order indices can be neglected for case 2, Table 6 shows that 256 samples are enough to obtain a correct ranking and 1024 samples are required to reach R = 99.99%. This result is same as the Weights result.

In summary, although these two methods are based on different algorithms, the PaD method is highly consistent with the variance-based methods and can acquire correct, accurate, and comprehensive evaluation results.

4.2. CH_4 model

In Section 4.1, two verification cases were calculated. In this part, a CH_4 model in which the true values cannot be obtained analytically was applied. For the Optimized-HDMR procedure, the maximum polynomial orders for the first and second order component functions were set as 5 and 3, respectively. The correlation method for the variance reduction was set as 10 for both the first and second component functions.

Table 7 lists the top five first and second order sensitivity indices calculated by the ANN-HDMR and PSO-BPNN-Wu methods with different sample sizes. It shows that 16,384 original samples are enough for the ANN-HDMR and PSO-BPNN-Wu methods to generate stable results. Additionally, for the ANN-HDMR method, the number of ANN samples also influenced the results.

Table 8 lists the sum ($S_i + S_{ij}$) and error using ANN-HDMR and ANN-DMC-HDMR (ANN with DMC-HDMR, which needs more samples but is more accurate). It shows that ANN-HDMR requires 0.2 million samples to reduce the error to below 5%, while ANN-DMC-HDMR requires 1.5 million. To reduce the error below 1% and have a sum ($S_i + S_{ij}$) < 1, 0.8 million and 12 million samples are required, respectively. Thus, the ANN sample size was set to 0.8 million in this case. Moreover, different from the above case, the sensitivity indices calculated using ANN-DMC-HDMR with 16,384 original samples and 12 million generated samples were taken as true reference values; the error values were also calculated based on these parameters. Furthermore, by comparing the ANN-HDMR and PSO-BPNN-Wu error in Table 7, the PSO-BPNN-Wu method converges faster than the ANN-HDMR method, which is similar to the discussion in Section 4.1. PSO-BPNN-Wu requires 8192 original samples to reduce the error to 1%, while ANN-HDMR needs 16,384 samples. Moreover, only 2048 original samples are needed for both methods to obtain acceptable ranking results. These results demonstrate that the convergence speed can be accelerated by introducing the ANN technology and that PSO-BPNN has better performance.

Results from the sensitivity analysis using the Weights and Pad method with different sample sizes are listed in Tables 9 and 10. Comparing Table 9 with Table 10, it is clear that sensitivity indices calculated using the Weights and PaD methods have high accordance with the HDMR results. Specifically, the Weights method requires 8192 samples to reach an R value above 95% and PaD method requires 4096 for both the first and second order sensitivity indices. Furthermore, only 2048 original samples are required for the PaD method to obtain a correct ranking for the first and second order sensitivity indices.

According to ranking, the most important reaction is reaction 158, whose first order term contributes 23% to the overall variance. The top 5 reactions together contribute approximately two-thirds of the delay time. For the second order sensitivity indices, the most important effect comes from (32,158). It is our mission to analyze the detailed reaction and its mechanism and to compare the results to different methods.

To compare the computational cost of the different methods, the total CPU time (TT) was introduced; it consists of the following two parts: 1) time to generate the original samples (TO) and 2) time to calculate the sensitivity indices (TS). Moreover, a speedup ratio (take DMC-HDMR with 6 million samples as a reference and divide by each method) was introduced to evaluate the accelerating performance. Table 11 lists the above parameters from the different methods. Because the typical DMC-HDMR and Optimized-HDMR methods without ANN require lots of original samples, estimated TO values are given; these values are estimated as follows: one original sample takes approximately 1 s in our platform, implying that approximately 1666.7 and 224 h are needed for the 6 million and 0.8 million samples, respectively. Additionally, the original sample sizes from the typical DMC-HDMR and Optimized-HDMR methods reference the generated sample size in the ANN-DMC-HDMR and ANN-HDMR methods. However, the practical demands may be considerably larger because the ANN can accelerate the convergence speed and decrease the required sample size (Li et al., 2016). Furthermore, ANN-HDMR takes approximately 71.0 h to obtain stable results and PSO-BPNN-Wu takes approximately 31.7 h, while the Weights and PaD method only takes approximately 20 min. Wu's method reduces the TT by half because it is an ANOVA-based optimization algorithm. Moreover, by comparing Table 8 with Table 11, DMC-HDMR requires 50.2 h and 6 million samples to reduce the error below 1%, while the Optimized-HDMR method only needs 71.0 h and 0.8 million samples to reduce the error below 1%. Hence, DMC-HDMR appears to be more effective and accurate than Optimized-HDMR. When an enormous number of samples can be generated effectively due to the strong ability of the PSO-BPNN (only takes 2 s to generate one million samples), the Optimized-HDMR with variance reduction algorithm increases rather than decreases the computational cost.

The required time for the Weights and PaD methods are just 1/1430 and 1/63 of the DMC-HDMR and ANN-HDMR methods, respectively. Because these two methods reduce both TO and TS, the cost is reduced several orders of magnitude. Moreover, it only requires 0.2 h to obtain both the Weights and PaD sensitivity indices. Hence, these two methods can be utilized together and decrease the possibility of error.

In this case, the results indicate that the new framework, especially the PSO-BPNN-Weights and -PaD methods, have computational cost reduction and error reduction advantages.

4.3. Applications

The new framework has been tested and analyzed in Sections 4.1 and 4.2. In this framework, the PSO-BPNN-Wu method can obtain the Sobol' sensitivity indices but costs much more CPU time, while the Weights and Pad methods are faster but cannot

Table 7
The important first and second order sensitivity indices for the CH_4/air system ignition delay time using ANN-HDMR and PSO-BPNN-Wu.

N	ANN-HDMR				PSO-BPNN-Wu			
	2048	4096	8192	16,384	2048	4096	8192	16,384
S_{158}	0.2348	0.2445	0.2471	0.2470	0.2419	0.2470	0.2472	0.2472
S_{156}	0.1511	0.1561	0.1574	0.1609	0.1549	0.1595	0.1608	0.1608
S_{32}	0.1114	0.1143	0.1151	0.1172	0.1135	0.1162	0.1174	0.1174
S_{119}	0.1023	0.1045	0.1049	0.1131	0.1040	0.1049	0.1133	0.1133
S_{53}	0.0490	0.0501	0.0504	0.0492	0.0499	0.0501	0.0491	0.0492
$\Sigma(S_i)$	0.7486	0.8095	0.8549	0.8647	0.7942	0.8626	0.8642	0.8640
$S_{32,158}$	0.0211	0.0102	0.0074	0.0072	0.0132	0.0071	0.0079	0.0078
$S_{119,158}$	0.0211	0.0102	0.0074	0.0071	0.0131	0.0071	0.0078	0.0075
$S_{32,156}$	0.0198	0.0095	0.0069	0.0065	0.0123	0.0066	0.0067	0.0067
$S_{156,158}$	0.0218	0.0106	0.0076	0.0054	0.0136	0.0060	0.0055	0.0057
$S_{119,156}$	0.0211	0.0109	0.0083	0.0056	0.0137	0.0048	0.0050	0.0051
$\Sigma(S_{i,j})$	0.1549	0.1014	0.0576	0.0949	0.1095	0.0932	0.0950	0.0956
$\Sigma(S_i + S_{i,j})$	0.9035	0.9109	0.9125	0.9556	0.9037	0.9558	0.9601	0.9594
Error	0.2216	0.0921	0.0242	0.0092	0.0772	0.0194	0.0079	0.0010

Table 8
The important first and second order sensitivity indices for the CH_4/air system ignition delay time vary based on the generated sample sizes using ANN-HDMR and ANN-DMC-HDMR.

N	ANN-HDMR				ANN-DMC-HDMR			
	0.1 M	0.2 M	0.4 M	0.8 M	1.50 M	3 M	6 M	12 M
$\Sigma(S_i)$	0.8688	0.8664	0.8649	0.8647	1.4786	0.8320	0.8641	0.8641
$\Sigma(S_{i,j})$	0.0868	0.0879	0.0896	0.0949	4.0808	0.2550	0.1003	0.0954
$\Sigma(S_i + S_{i,j})$	0.9556	0.9543	0.9545	0.9556	5.5594	1.087	0.9644	0.9595
Error	0.0577	0.0448	0.0313	0.0092	4.7045	0.0197	0.0081	0.0000

Table 9
The important first and second order sensitivity indices for the CH_4/air system ignition delay time using the PSO-BPNN-Weights. The total variance contribution indices obtained using ANN-DMC-HDMR were used as reference values.

N	PSO-BPNN-Weights				ANN-DMC-HDMR
	1024	2048	4096	8192	
S_{T158}	0.0313	0.0314	0.0273	0.0249	0.2607
S_{T156}	0.0257	0.0256	0.0217	0.0212	0.1739
S_{T32}	0.0254	0.0230	0.0191	0.0212	0.1293
S_{T119}	0.0211	0.0228	0.0189	0.0187	0.1237
S_{T53}	0.0215	0.0181	0.0154	0.0142	0.0515
R	0.7152	0.8599	0.9694	0.9892	1.0000

Table 10
The important first and second order sensitivity indices for the CH_4/air system ignition delay time using the PSO-BPNN-PaD. The sensitivity indices obtained using ANN-DMC-HDMR were used as reference values.

N	PSO-BPNN-PAD				ANN-DMC-HDMR
	1024	2048	4096	8192	
S_{158}	0.3119	0.2077	0.2383	0.2338	0.2473
S_{156}	0.1421	0.1030	0.0755	0.0755	0.1608
S_{32}	0.1025	0.1015	0.0625	0.0617	0.1173
S_{119}	0.0831	0.0738	0.0612	0.0617	0.1133
S_{53}	0.0632	0.0472	0.0386	0.0382	0.0492
R	0.9807	0.9864	0.9906	0.9965	1.0000
$S_{32,158}$	0.0139	0.0282	0.0212	0.0210	0.0077
$S_{119,158}$	0.0101	0.0245	0.0113	0.0113	0.0075
$S_{32,156}$	0.0080	0.0186	0.0098	0.0097	0.0067
$S_{156,158}$	0.0147	0.0124	0.0076	0.0075	0.0057
$S_{119,156}$	0.0067	0.0101	0.0076	0.0074	0.0050
R	0.8130	0.9041	0.9583	0.9712	1.0000

obtain the Sobol' sensitivity indices. Furthermore, due to the powerful computational ability of the new framework, the sensitivity indices of more complex models can be easily implemented. To achieve this target, the following four-step process combining the advantages of the different methods was proposed:

1) Generating original samples using chemical kinetic programs;
2) Training the PSO-BPNN;
3) Using the Weights and PaD method to obtain the sensitivity indices and ranking; and
4) (Optional) Calculating the Sobol' sensitivity indices of the most remarkable inputs (such as the top 5) using Wu's method and verifying the results obtained in step 3.

By following these four steps, we can obtain reliable sensitivity index and sensitivity ranking results. A C_2H_4 chemical kinetic model including 111 species and 784 reversible reactions updated by Wang et al., (2007) was applied (Wang), and a detailed model

Table 11
Computational cost of the different methods. TT represents the total CPU time, TO represents the time to generate the original samples, and TS represents the time to calculate the sensitivity indices.

Time (hours)	DMC-HDMR	Optimized-HDMR	ANN-DMC- HDMR	ANN-HDMR	PSO-BPNN-Wu	PSO-BPNN-Weights & PaD
	6 M	0.8 M	16,384	16,384	8192	8192
TO	1666.7	224	4.6	4.6	2.3	2.3
TS	50.2	71.0	50.2	71.0	29.4	0.2
TT	1716.9	295.6	54.8	75.6	31.7	1.2
Speedup	1.0	5.8	31.3	22.7	54.2	1430.1

Table 12
The important first and second order sensitivity indices for the C_2H_4/air system ignition delay time obtained by following the four-step process.

N	PSO-BPNN-Weights				PSO-BPNN-PaD				PSO-BPNN-Wu
	2048	4096	8192	16384	2048	4096	8192	16,384	16,384
S_{194}	0.0234	0.0240	0.0262	0.0275	0.3800	0.3211	0.3190	0.3132	0.3795
S_{195}	0.0179	0.0185	0.0202	0.0210	0.2719	0.3031	0.3044	0.3013	0.2716
S_{266}	0.0145	0.0143	0.0160	0.0170	0.1519	0.1264	0.1259	0.1233	0.1512
S_{251}	0.0061	0.0074	0.0105	0.0113	0.0226	0.0317	0.0312	0.0305	0.0164
S_{252}	0.0078	0.0072	0.0098	0.0105	0.0169	0.0260	0.0255	0.0244	0.0152
$S_{194,195}$					0.0149	0.1210	0.0813	0.0827	0.0076
$S_{194,266}$					0.0521	0.0804	0.0546	0.0535	0.0032
$S_{195,266}$					0.0888	0.0474	0.0322	0.0323	0.0025
$S_{14,194}$					0.1327	0.0135	0.0092	0.0090	0.0021
$S_{14,195}$					0.0101	0.0095	0.0067	0.0067	0.0019

can be found in Supplementary Materials S3. In Table 12, the sensitivity indices were obtained by following the four-step process. It shows that only 16,384 original samples were needed for the Weights and PaD method to obtain a stable result, and 15 h were needed to finish all the calculations. Furthermore, if only a correct ranking was required, 4096 samples and 4 h could give perfectly acceptable results.

5. Conclusions

This work presents a new framework that combines variance- and ANN-based sensitivity analysis methods. Particularly, a PSO-BPNN was introduced as a core to replace HDMR and perform global sensitivity analysis, which mainly includes the following two aspects. First, Wu's method was introduced to calculate the variance-based sensitivity indices-Sobol' sensitivity indices using generated samples from a PSO-BPNN, namely, the PSO-BPNN-Wu. Second, the Weights and PaD methods were used to obtain ANN-based global sensitivity indices via PSO-BPNN-Weights and PSO-BPNN-PaD, which were highly correlated with Sobol' sensitivity indices. Using the Sobol' g-function and a methane reaction kinetic model in ignition as test cases, the proposed PSO-BPNN-Wu has been proven to have great accuracy. Additionally, the PSO-BPNN-Weights and PaD methods can greatly reduce the computational cost by two orders of magnitude. Furthermore, to couple the advantages of these three methods, a four-step process was presented and has been applied to a detailed C_2H_4 chemical kinetic model. The sensitivity indices of the more complex models can be implemented easily and affordably by following this four-step process in future work.

Acknowledgments

This work was financially supported by the National Natural Science Foundation of China (Contract no. 51376152 and no. 91541110).

Supplementary materials

Supplementary material associated with this article can be found, in the online version, at doi:10.1016/j.compchemeng.2018.02.003.

References

Ahmad, A.L., Azid, I.A., Yusof, A.R., Seetharamu, K.N., 2004. Emission control in palm oil mills using artificial neural network and genetic algorithm. Comput. Chem. Eng. 28, 2709–2715.
Ali, J.M., Hoang, N.H., Hussain, M.A., Dochain, D., 2015. Review and classification of recent observers applied in chemical process systems. Comput. Chem. Eng. 76, 27–41.
Alis, O.F., Rabitz, H., 2001. Efficient implementation of high dimensional model representations. J. Math. Chem. 29, 127–142.
Balls, G.R., Palmer-Brown, D., Sanders, G.E., 1996. Investigating microclimatic influences on ozone injury in clover (Trifolium subterraneum) using artificial neural networks. New Phytol 132, 271–280.
Borgonovo, E., 2007. A new uncertainty importance measure. Reliab. Eng. Syst. Saf. 92, 771–784.
Cao, J., Cui, H., Shi, H., Jiao, L., 2016. Big data: a parallel particle swarm optimization-back-propagation neural network algorithm based on MapReduce. PLoS One 11, e0157551.
Cao, M., Qiao, P., 2007. Neural network committee-based sensitivity analysis strategy for geotechnical engineering problems. Neural Comput. Appl. 17, 509–519.
Chun, M.H., Han, S.J., Tak, N.I., 2000. An uncertainty importance measure using a distance metric for the change in a cumulative distribution function. Reliab. Eng. Syst. Saf. 70, 313–321.
Cui, L., Xie, P., Sun, J., Yu, T., Yuan, J., 2012. Data-driven prediction of the product formation in industrial 2-keto-L-gulonic acid fermentation. Comput. Chem. Eng. 36, 386–391.
Da, Y., Ge, X., 2005. An improved PSO-based ANN with simulated annealing technique. Neurocomputing 63, 527–533.
Dimopoulos, I., Chronopoulos, J., Chronopoulou-Sereli, A., Lek, S., 1999. Neural network models to study relationships between lead concentration in grasses and permanent urban descriptors in Athens city (Greece). Ecol. Model. 120, 157–165.
Dimopoulos, Y., Bourret, P., Lek, S., 1995. Use of some sensitivity criteria for choosing networks with good generalization ability. Neural Process. Lett. 2, 1–4.
Ferreira, C., 2006. Designing Neural Networks Using Gene Expression Programming. Springer, Berlin Heidelberg.
Garson, G.D., 2012. Interpreting neural-network connection weights. Ai Expert 6, 46–51.
Geethanjali, M., Raja Slochanal, S.M., Bhavani, R., 2008. PSO trained ANN-based differential protection scheme for power transformers. Neurocomputing 71, 904–918.
Gevrey, M., Dimopoulos, I., Lek, S., 2003. Review and comparison of methods to study the contribution of variables in artificial neural network models. Ecol. Model. 160, 249–264.
Gevrey, M., Dimopoulos, I., Lek, S., 2006. Two-way interaction of input variables in the sensitivity analysis of neural network models. Ecol. Model. 195, 43–50.
Haaker, M.P.R., Verheijen, P.J.T., 2004. Local and global sensitivity analysis for a reactor design with parameter uncertainty. Chem. Eng. Res. Des. 82, 591–598.
Hao, W.R., Lu, Z.Z., Wei, P.F., Feng, J., Wang, B.T., 2012. A new method on ANN for variance based importance measure analysis of correlated input variables. Struct. Saf. 38, 56–63.
Lee, K.Y., Chung, N., Hwang, S., 2015. Application of an artificial neural network (ANN) model for predicting mosquito abundances in urban areas. Ecol. Inf.
Li, Wang, S.W., Rabitz, H., 2002. Practical approaches to construct RS-HDMR component functions. J. Phys. Chem. A 106, 8721–8733.
Li, G.Y., Rabitz, H., 2006. Ratio control variate method for efficiently determining high-dimensional model representations. J. Comput. Chem. 27, 1112–1118.
Li, G.Y., Rabitz, H., Wang, S.W., Georgopoulos, P.G., 2003. Correlation method for variance reduction of Monte Carlo integration in RS-HDMR. J. Comput. Chem. 24, 277–283.
Li, S., Yang, B., Qi, F., 2016. Accelerate global sensitivity analysis using artificial neural network algorithm: Case studies for combustion kinetic model. Combust. Flame 168, 53–64.
Lin, Z., Chen, G., Guo, W., Liu, Y., 2008. PSO-BPNN-based prediction of network security situation. In: Proceedings of the International Conference on Innovative Computing Information and Control, p. 37.
Liu, H., Chen, W., Sudjianto, A., 2006. Relative Entropy based method for probabilistic sensitivity analysis in engineering design. J. Mech. Des. 128, 326–336.
McKay, M.D., 1997. Nonparametric variance-based methods of assessing uncertainty importance. Reliab. Eng. Syst. Saf. 57, 267–279.
Nourani, V., Sayyah Fard, M., 2012. Sensitivity analysis of the artificial neural network outputs in simulation of the evaporation process at different climatologic regimes. Adv. Eng. Software 47, 127–146.

Olden, J.D., Joy, M.K., Death, R.G., 2004. An accurate comparison of methods for quantifying variable importance in artificial neural networks using simulated data. Ecol. Model. 178, 389–397.
Paruggia, M., 2006. Sensitivity analysis in practice: a guide to assessing scientific models. J. Am. Soc. Stat. Assoc. 101, 398–399.
Rabitz, H., Alis, O.F., 1999. General foundations of high-dimensional model representations. J. Math. Chem. 25, 197–233.
Rigo, D.D., Castelletti, A., Rizzoli, A.E., Soncini-Sessa, R., Weber, E., 2005. A selective improvement technique for fastening neuro-dynamic programming in water resource network. In: Proceedings of the IFAC World Congress. Prague, pp. 7–12.
Ruiz, D., Canton, J., Nougues, J.M., Espuna, A., Puigjaner, L., 2001. On-line fault diagnosis system support for reactive scheduling in multipurpose batch chemical plants. Comput. Chem. Eng. 25, 829–837.
Rumelhart, D.E., Hinton, G.E., Williams, R.J., 1986. Learning representations by back--propagating errors. Nature 323, 533–536.
Saltelli, A., Sobol, I.M., 1995. About the use of rank transformation in sensitivity analysis of model output. Reliab. Eng. Syst. Saf. 50, 225–239.
Scardi, M., Harding Jr., L.W., 1999. Developing an empirical model of phytoplankton primary production: a neural network case study. Ecol. Model. 120, 213–223.
Sellitto, P., 2017. Artificial Neural Networks for Spectral Sensitivity Analysis to Optimize Inversion Algorithms for Satellite-Based Earth Observation: Sulfate Aerosol Observations With High-Resolution Thermal Infrared Sounders A2 - Petropoulos. In: George, P., Srivastava, P.K. (Eds.), Sensitivity Analysis in Earth Observation Modelling. Elsevier, pp. 161–175.
Sikorski, J.J., Brownbridge, G., Garud, S.S., Mosbach, S., Karimi, I.A., Kraft, M., 2016. Parameterisation of a biodiesel plant process flow sheet model. Comput. Chem. Eng. 95, 108–122.
Smith, G.P., Golden, D.M., Frenklach, M., Moriarty, N.W., E., B., Golden-borg, M., Bowman, C.T., Hanson, R.K., Song, S., Gardiner, W.C., Lissianski, V.V., Qin, Z. GRI_MECH 3.0 http://www.me.berkeley.edu/gri_mech/ (accessed March 2016).
Sobol, I.M., 1990. Sensitivity estimates for nonlinear mathematical models. Matem Mod 2, 112–118.
Sobol, I.M., 2001. Global sensitivity indices for nonlinear mathematical models and their Monte Carlo estimates. Math. Comput. Simulat. 55, 271–280.
Wang, H., You, X., Joshi, A.V., Davis, S.G., Laskin, A., Egolfopoulos, F.N., Law, C.K. USC mech version II. High-temperature combustion reaction model of H2/CO/C1-C4 compounds http://ignis.usc.edu/Mechanisms/USC-Mech%20II/USC_Mech%20II.htm (accessed March 2016).
Wu, Q.-L., Cournède, P.-H., Mathieu, A., 2012. An efficient computational method for global sensitivity analysis and its application to tree growth modelling. Reliab. Eng. Syst. Saf. 107, 35–43.
Xiao, W.P., Ye, J.W., 2009. Improved PSO-BPNN algorithm for SRG modeling. In: Proceedings of the International Conference on Industrial Mechatronics and Automation, pp. 245–248.
Ziehn, T., Tomlin, A.S., 2008a. Global sensitivity analysis of a 3D street canyon model—Part I: the development of high dimensional model representations. Atmos. Environ. 42, 1857–1873.
Ziehn, T., Tomlin, A.S., 2008b. A global sensitivity study of sulfur chemistry in a premixed methane flame model using HDMR. Int. J. Chem. Kinet. 40, 742–753.
Ziehn, T., Tomlin, A.S., 2009. GUI-HDMR - a software tool for global sensitivity analysis of complex models. Environ. Model. Software 24, 775–785.
Zorzetto, L.F.M., Maciel, R., Wolf-Maciel, M.R., 2000. Process modelling development through artificial neural networks and hybrid models. Comput. Chem. Eng. 24, 1355–1360.